Int. J. Heat Mass Transfer. Vol. 13, pp. 434–438. Pergamon Press 1970. Printed in Great Britain

COMBINED FORCED AND FREE CONVECTION FLOW ON VERTICAL SURFACES

J. R. LLOYD and E. M. SPARROW
Department of Mechanical Engineering, University of Minnesota, Minneapolis, Minnesota

(*Received* 19 *May* 1969 *and in revised form* 22 *September* 1969)

NOMENCLATURE

f, reduced stream function, $\psi/\sqrt{(U_\infty \nu x)}$;
Gr_x, Grashof number, $g\beta(T_w - T_\infty)x^3/\nu^2$;
g, acceleration of gravity;
h, local heat-transfer coefficient, $q/(T_w - T_\infty)$;
k, thermal conductivity;
Nu_x, local Nusselt number, hx/k;
Pr, Prandtl number;
q, local heat-transfer per unit time and area;
Re_x, Reynolds, number, U_∞/ν;
T, temperature;
T_w, wall temperature;
T_∞, ambient temperature;
U_∞, free stream velocity;
x, streamwise coordinate;
y, transverse coordinate;
β, thermal expansion coefficient;
η, pseudo-similarity variable, equation (1);
θ, temperature variable, $(T - T_\infty)/(T_w - T_\infty)$;
ν, kinematic viscosity;
ξ, transformed streamwise coordinate, equation (1);
ψ, stream function.

INTRODUCTION

THIS note is concerned with aiding forced and free convection flows adjacent to an isothermal vertical plate. This problem does not admit similarity solutions. Approximate solutions, appropriate to small buoyancy effects, have been obtained in terms of series expansions about the basic forced convection flow [1, 2]. Earlier attempts [1, 3] to construct series solutions about the free convection flow have recently been shown to be in error [4]. In [4], a complete solution, numerically applicable to $Pr = 1$, is obtained by a combination of series expansion and numerical integration. A solution based on the approximate Karman–Pohlhausen method is also available [5], but the results have been found to be substantially in error [6]. In [6], consideration is given to the limits of $Pr \to 0$ and $Pr \to \infty$, and results are presented for the stagnation region of a horizontal cylinder. The only relevant experiments appear to be those of Kliegel [7] which pertain to a vertical plate situated in an air stream.

In the present investigation, the method of local similarity is applied. The solutions thus obtained encompass conditions ranging from pure forced convection flow to combined flows with strong free convection contributions. Numerical results are presented for Prandtl numbers of 0·003, 0·01, 0·03, 0·72, 10 and 100, thereby providing detailed information for liquid metals as well as for gases and ordinary liquids.

ANALYSIS

The coordinate system and other nomenclature are shown at the upper left of Fig. 1, where, for aiding forced and free convection flows, $T_w > T_\infty$. The analysis is also applicable when U_∞ is downward, $T_w < T_\infty$, and x is measured in the downward direction.

The starting point of the analysis is the conservation equations for mass, momentum and energy. As a first step in the local similarity solution, the coordinates are transformed from the (x, y) system to the (ξ, η) system, where $\eta = \eta(x, y)$ and $\xi = \xi(x)$. The coordinate η, termed a pseudo-similarity variable, serves the function of suppressing the x-dependence associated with the normal streamwise development of the boundary layer, that is, the x-dependence encountered in similarity boundary layers. Thus, subsequent to the transformation, the remaining dependence on the streamwise coordinate is that due to the non-similarity alone.

For the definitions of η and ξ, we take

$$\eta = y\sqrt{\left(\frac{U_\infty}{\nu x}\right)}, \qquad \xi = \frac{g\beta(T_w - T_\infty)x^3/\nu^2}{U_\infty^2 x^2/\nu^2} = \frac{Gr_x}{Re_x^2} \sim x. \quad (1)$$

It is seen that η is identical to the similarity variable for the forced convection boundary layer, while ξ is a dimensionless rephrasing of x itself which also serves as an index of the relative contributions of forced convection and free convection. In addition to the new coordinates defined by equation (1), new dependent variables $f(\xi, \eta)$ and $\theta(\xi, \eta)$, respectively representing the reduced stream function and reduced temperature, are introduced, where the choice of the reduced stream function f is made to complement the foregoing choice of η.

The formal transformation of the conservation equations can thus be carried out. Then, in accordance with the principle of local similarity, the ξ derivatives are deleted

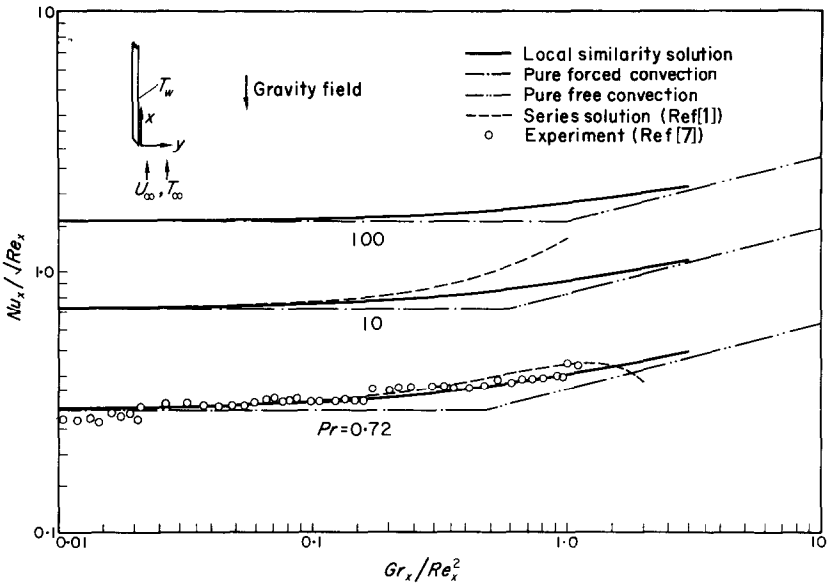
Local similarity solution
Pure forced convection
Pure free convection
Series solution (Ref[1])
Experiment (Ref[7])
Gravity field
T_w
x
y
U_∞, T_∞
100
10
Pr=0·72
$Nu_x/\sqrt{Re_x}$
Gr_x/Re_x^2
10
1·0
0·1
0·01
0·1
1·0
10

FIG. 1.

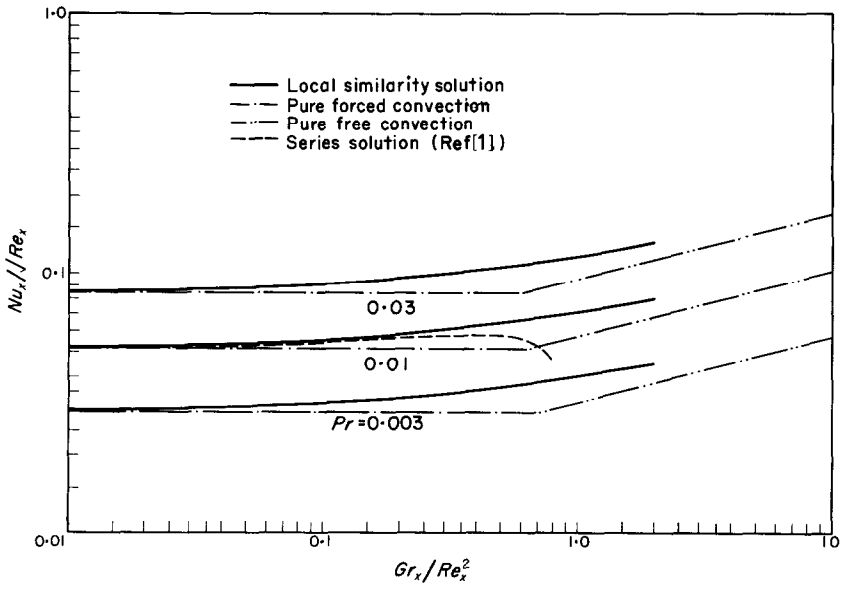
Local similarity solution
Pure forced convection
Pure free convection
Series solution (Ref[1])
0·03
0·01
Pr=0·003
Nu_x/Re_x
Gr_x/Re_x^2
1·0
0·1
0·01
0·1
1·0
10

FIG. 2.

from the thus-transformed equations. The end result of these operations is

$$\frac{\partial^3 f}{\partial \eta^3} + \tfrac{1}{2} f \frac{\partial^2 f}{\partial \eta^2} + \xi\theta = 0, \qquad \frac{\partial^2 \theta}{\partial \eta^2} + \tfrac{1}{2} Prf \frac{\partial \theta}{\partial \eta} = 0 \quad (2)$$

subject to the boundary conditions

$$f(\xi, 0) = \left(\frac{\partial f}{\partial \eta}\right)_{\xi, 0} = 0, \qquad \theta(\xi, 0) = 1,$$

$$\left(\frac{\partial f}{\partial \eta}\right)_{\xi, \infty} = 1, \qquad \theta(\xi, \infty) = 0. \quad (3)$$

At any streamwise position along the plate, the quantity $\xi (= Gr_x/Re_x^2)$ may be regarded as an assignable constant parameter. As a consequence, equations (2) and (3) may be treated as a system of ordinary differential equations at each streamwise location of interest, with numerical solutions being obtained by methods used for similarity boundary layers.

Solutions have been carried out for Prandtl numbers ranging from 0·003 to 100. For each Pr, the quantity Gr_x/Re_x^2 was varied from 0 to 2–4, thus spanning the range from pure forced convection to strong (sometimes dominant) buoyancy effects.

RESULTS AND DISCUSSION

In terms of the variables of the analysis, the local Nusselt number may be expressed as $Nu_x/\sqrt{Re_x} = -(\partial\theta/\partial\eta)_{\xi, 0}$. The thus-determined values of $Nu_x/\sqrt{Re_x}$ are plotted as solid lines in Figs. 1 and 2, which, respectively, contain results for $Pr = 0{\cdot}72$, 10 and 100 (gases and ordinary liquids) and for $Pr = 0{\cdot}003$, 0·01 and 0·03 (liquid metals). The magnitude of the abscissa variable Gr_x/Re_x^2 is an index of the relative importance of the free convection and forced convection contributions. In addition to the local similarity results, the figures also contain straight lines which represent $Nu_x/\sqrt{Re_x}$ for pure forced convection flow and for pure free convection flow. The dashed lines and the experimental data that appear in the figures will be discussed later. A listing of Nu_x/Re_x is also given in Table 1 to facilitate future application.

Inspection of Figs. 1 and 2 reveals trends that are common to all of the Prandtl numbers investigated. At small values of Gr_x/Re_x^2, the Nusselt number results (solid lines) merge smoothly with the asymptotes for pure forced convection. As the free convection grows relatively stronger (i.e. increasing values of Gr_x/Re_x^2), $Nu_x/\sqrt{Re_x}$ increases monotonically, deviating more and more from the respective forced convection asymptotes. At still larger values of Gr_x/Re_x^2, the Nusselt number results tend to approach the asymptotes for pure free convection. Thus, at any value of Gr_x/Re_x^2, the Nusselt number in an aiding combined forced and free convection flow is higher than it would be in either of the component flows.

The greatest deviations of the Nusselt number results (solid lines) from the envelope curve formed by the forced convection and free convection asymptotes occur at the intersection of the asymptotes. These deviations are approximately 15 per cent for $Pr = 100$ and 10; 19 per cent for $Pr = 0{\cdot}72$; and 22 per cent for $Pr = 0{\cdot}03$, 0·01 and 0·003.

One can also determine the value of Gr_x/Re_x^2 at which significant deviations of the Nusselt number from its forced convection value first occur. If a 5 per cent deviation is taken as the threshold of significant effects, then the corresponding threshold values of Gr_x/Re_x^2 are 0·24, 0·13, 0·08 and 0·056–0·05, respectively for $Pr = 100$, 10, 0·72 and 0·03–0·003. These findings show the greater sensitivity of low Prandtl number flows to buoyancy effects.

The data of Kliegel [7] are, apart from scatter, in very good agreement with the results of the present analysis, thereby lending support to the analytical method. The dashed lines appearing in the figures represent series solutions, the first term of the series being that for forced convection flow. The results from the series solutions display reasonable trends for small values of Gr_x/Re_x^2, but appear to diverge for moderate and large values of this parameter.

Representative velocity and temperature profiles. In Figs. 3, 4 and 5, the velocity profiles are referred to the left-hand

Table 1. *Values of* $Nu_x/\sqrt{Re_x}$

	Pr					
Gr_x/Re_x^2	0·003	0·01	0·03	0·72	10	100
0·0	0·02937	0·05159	0·08439	0·2956	0·7281	1·572
0·01	0·02966	0·05210	0·08524	0·2979	0·7313	1·575
0·04	0·03040	0·05346	0·08750	0·3044	0·7404	1·585
0·1	0·03160	0·05565	0·09118	0·3158	0·7574	1·605
0·4	0·03546	0·06264	0·1030	0·3561	0·8259	1·691
1·0	0·04000	0·07079	0·1168	0·4058	0·9212	1·826
2·0	0·04479	0·07936	0·1311	0·4584	1·029	1·994
4·0			0·1495	0·5258	1·173	2·232

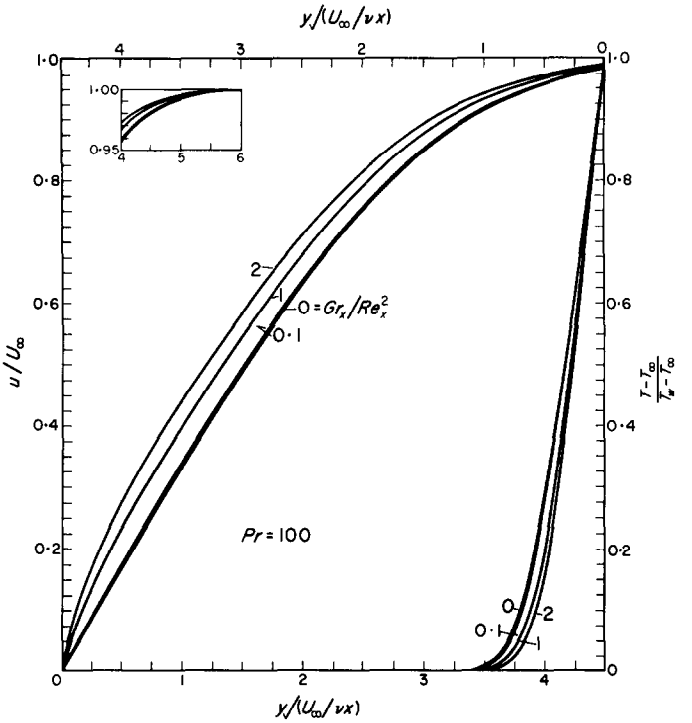
$y\sqrt{(U_\infty/\nu x)}$
u/U_∞
$\frac{T-T_\infty}{T_w-T_\infty}$
Gr_x/Re_x^2
Pr = 100

FIG. 3.

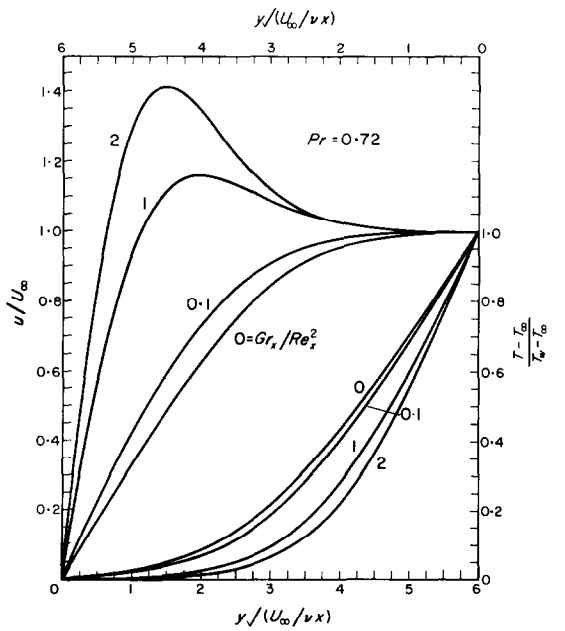
$y\sqrt{(U_\infty/\nu x)}$
u/U_∞
$\frac{T-T_\infty}{T_w-T_\infty}$
Gr_x/Re_x^2
Pr = 0·72

FIG. 4.

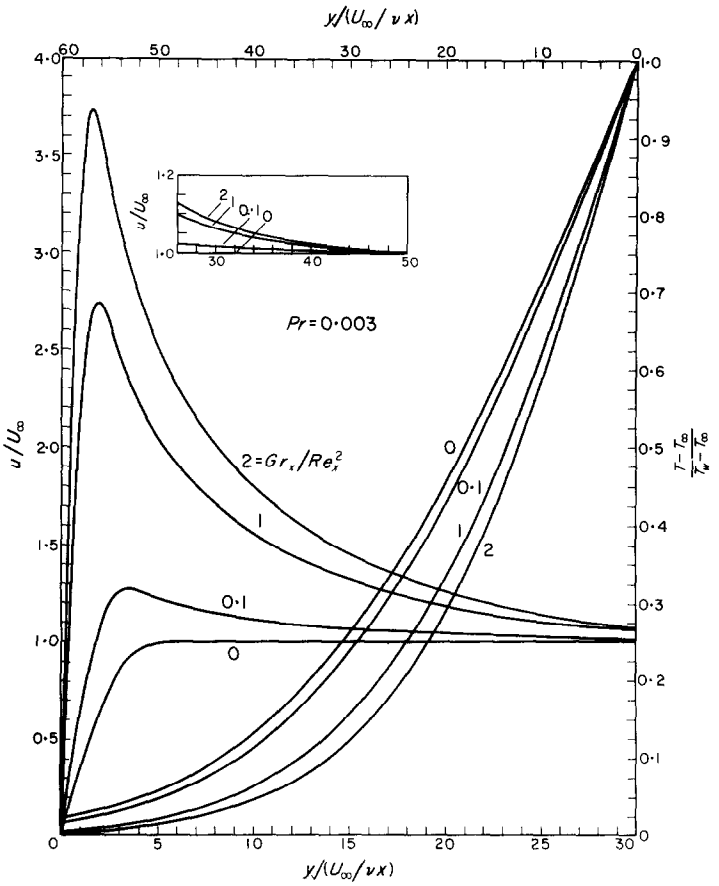

FIG. 5.

ordinate and lower abscissa, while the temperature profiles are referred to the right-hand ordinate and upper abscissa. From the figures, it is seen that the effect of buoyancy on the velocity distribution is markedly different at different Prandtl numbers, while the temperature profiles are affected in a qualitatively similar manner for all Prandtl numbers.

Turning to the velocity field, it may be observed that aside from a somewhat more rapid rise near the wall, the buoyancy-affected profiles for $Pr = 100$ are similar to those for pure forced convection (Fig. 3). For $Pr = 0{\cdot}72$ (Fig. 4), the presence of buoyancy results in a relatively sharp rise in the profile near the wall and a moderate overshoot (approximately 40 per cent) of the velocity beyond its free stream value. These effects are strongly accentuated at $Pr = 0{\cdot}003$, where the maximum velocity in the boundary layer is several times greater than that in the free stream (Fig. 5).

CONCLUDING REMARKS

The local similarity model used here is not applicable in the limit of large ξ. Therefore, an alternate local similarity analysis was tried in which η and f were, respectively, the free-convection similarity variable and reduced stream function, and $\xi = Re_x^2/Gr_x$. After execution of the transformation, it is found that the deletion of terms called for by the local similarity concept is in conflict with the boundary condition $u = U_\infty$ at $y = \infty$. Therefore, the local similarity model is not applicable in this case.

REFERENCES

1. A. A. SZEWCZYK, *J. Heat Transfer* **C86**, 501–507 (1964).
2. E. M. SPARROW and J. L. GREGG, *J. Appl. Mech.* **26**, 133–134 (1959).
3. S. ESHGHY, *J. Heat Transfer* **C86**, 290–291 (1964).
4. J. H. MERKIN, *J. Fluid Mech.* **35**, 439–450 (1969).
5. A. ACRIVOS, *A.I.Ch.E.Jl* **4**, 285–289 (1958).
6. A. ACRIVOS, *Chem. Engng Sci.* **21**, 343–352 (1966).
7. J. R. KLIEGEL, Laminar free and forced convection heat transfer from a vertical flat plate, Ph.D. Thesis University of California (1959).